



Published in final edited form as:

Angew Chem Int Ed Engl. 2019 June 17; 58(25): 8394–8399. doi:10.1002/anie.201901571.

Biosynthesis of L-4-Chlorokynurenine, a Lipopeptide Antibiotic Non-Proteinogenic Amino Acid and Antidepressant Prodrug

Hanna Luhavaya^a, Renata Sigrist^{a,b}, Jonathan R. Chekan^a, Shaun M. K. McKinnie^a, and Bradley S. Moore^{a,c}

^aCenter for Marine Biotechnology and Biomedicine, Scripps Institution of Oceanography, University of California, San Diego, La Jolla, CA 92093 (USA)

^bDepartment of Organic Chemistry, University of Campinas UNICAMP, Cidade Universitária Zeferino Vaz s/n, P.O. Box 6154, 13083-970, Campinas-SP (Brazil)

^cSkaggs School of Pharmacy and Pharmaceutical Sciences, University of California, San Diego, La Jolla, CA 92093 (USA)

Abstract

L-4-Chlorokynurenine (L-4-Cl-Kyn) is a neuropharmaceutical drug candidate in development for the treatment of major depressive disorder. Recently, this amino acid was naturally found as a residue in the lipopeptide antibiotic taromycin. Herein we report the unprecedented conversion of L-tryptophan to L-4-Cl-Kyn catalyzed by four enzymes in the taromycin biosynthetic pathway from the marine bacterium *Saccharomonospora* sp. CNQ-490. We used genetic, biochemical, structural, and analytical techniques to establish L-4-Cl-Kyn biosynthesis, which is initiated by the Tar14 flavin-dependent tryptophan chlorinase and its flavin reductase partner Tar15. This work revealed the first tryptophan 2,3-dioxygenase (Tar13) and kynurenine formamidase (Tar16) enzymes that are selective for chlorinated substrates. The substrate scope of Tar13, 14, and 16 was examined revealing intriguing promiscuity, thereby opening doors for the targeted engineering of these enzymes as useful biocatalysts.

Graphical Abstract

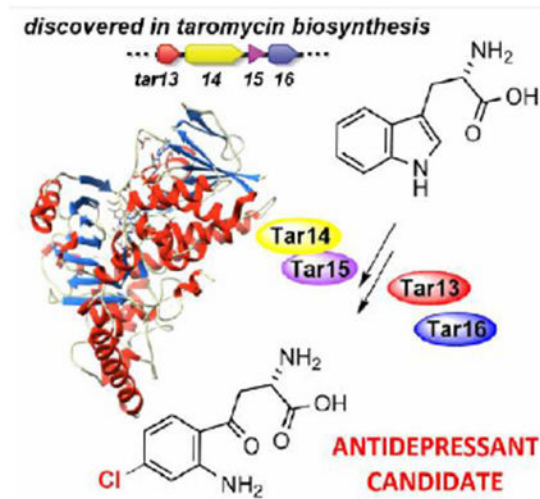
Supporting information for this article is given via a link at the end of the document.

Experimental Section

Experimental Details are given in the Supporting Information online.

Conflict of Interest

The authors declare no conflict of interest.



Two paths diverge: The unique enzymatic route to neuroactive L-4-chlorokynurenine has been revealed using a blend of in vitro experiments, X-ray crystallography, and CRISPR/Cas9-mediated gene deletion. Tar13 and Tar16 are the first tryptophan 2,3-dioxygenase and kynurenine formamidase homologs, respectively, to preferentially accept chlorinated substrates. Enzymes characterized here are promising candidates for chemoenzymatic synthesis.

Keywords

biocatalysis; biosynthesis; chlorokynurenine; halogenation; natural product

Non-proteinogenic amino acid L-4-chlorokynurenine (L-4-Cl-Kyn, **1**) is a next-generation, fast-acting oral prodrug for the treatment of major depressive disorder.^[1,2] Additional studies report that this drug candidate is effective in animal models for the treatment of neuropathic pain, epilepsy, and Huntington's disease.^[2] After active transport across the blood-brain barrier, **1** is enzymatically converted into the active agent 7-chlorokynurenic acid, which is a highly selective competitive antagonist of the *N*-methyl-D-aspartic acid (NMDA) receptor.^[3] To date, only synthetic routes to **1** have been described.^[3,4]

Biologically, **1** was recently identified as an amino acid building block in the lipopeptide antibiotics taromycin A (**2**) and B (**3**) (Figure 1A)^[5,6] and in the putative glycopeptide antibiotic complex INA-5812.^[7] With the concurrent discovery of the taromycin biosynthetic gene cluster (BGC) from the marine actinomycete *Saccharomonospora* sp. CNQ-490, we sought to establish the biosynthetic logic for the bacterial synthesis of L-4-Cl-Kyn. Herein we report the concise three-step L-4-Cl-Kyn pathway originating from L-tryptophan (L-Trp, **4**) and present it as an orthogonal approach to produce this promising drug candidate.

Enzymatic conversion of L-Trp to L-kynurenine (L-Kyn, **5**) is part of the kynurenine pathway (Figure 1B), the major Trp catabolic pathway in eukaryotes, which leads to vital biochemicals such as the neuroinhibitor kynurenic acid and the cofactor NADH.^[8] The

initial and rate-limiting step of the pathway is catalyzed by the Fe²⁺/heme-dependent enzyme tryptophan-2,3-dioxygenase (TDO) leading to formation of *N*-formyl-L-Kyn (**6**), which is hydrolyzed by kynurenine formamidase (KF) to give L-Kyn. Considering the functional importance of the products of this pathway, TDOs and KFs show specificity for L-Trp and *N*-formyl-L-Kyn, respectively. Homologous enzymes have been identified in some prokaryotes,^[9] however, they are not essential for bacterial survival, as bacteria catabolize Trp mainly through non-oxidative degradation.^[10] Recently, BGCs with co-clustered TDO-encoding genes have been discovered, but in vitro studies of these enzymes remain limited. Cluster-specific TDOs have been shown to have broader substrate specificities (*e.g.*, the actinomycin TDO AcnG accepts L-Trp, D/L- α -CH₃-Trp, D/L-5-CH₃-Trp, and D/L-5-F-Trp).^[11–14] Only one representative of a BGC-associated KF, from actinomycin biosynthesis, has been tested in vitro.^[15] This enzyme predominantly worked on *N*-formyl-L-Kyn, but was also able to deformylate at reduced rates *N',N*- α -diformyl-L-Kyn and *O*-formamino acetophenone. Bioinformatic analysis of the taromycin BGC (*tar*) identified an unprecedented quartet of enzymes – Tar13, 14, 15, and 16 – that show close homology to TDO, flavin-dependent halogenase (FDH), flavin reductase, and KF, respectively, and are encoded by adjacent genes (Figure 1C).

Considering that taromycin contains a second chlorinated amino acid residue, L-6-Cl-Trp (**7**), and that its BGC encodes only one halogenase, we hypothesized that the chlorination reaction takes place directly on L-Trp versus on a carrier protein bound substrate^[16] or post-assembly on a released peptide substrate.^[17] Phylogenetic analysis of Tar14 showed that it clades with FDHs acting on free L-Trp (Figure S1). To validate this, we performed an in-frame gene deletion of *tar14*. The availability of the 62.4 kb *tar* BGC cloned in pCAP01-*tarM1*^[6] allowed rapid genetic interrogations of the pathway. The *tar* cluster showed instability upon use of recombineering techniques, therefore, we chose an in vitro CRISPR/Cas9 approach (Figure S9).^[18] The deletion construct, pCAP01-*tarM1 tar14*, was integrated into the genome of *Streptomyces coelicolor* M1146 for heterologous expression.^[19] Liquid chromatography mass spectrometry (LCMS) analysis of the mutant culture extracts revealed abolished production of **2** and **3** (Figure 2A). Chemical complementation of the mutant strain with 6-Cl-Trp restored taromycin production. These results validated that free L-Trp is the substrate for Tar14, and strongly suggested that L-4-Cl-Kyn is formed by conversion of L-6-Cl-Trp rather than direct halogenation of L-Kyn.

Next, we proceeded with the in vitro reconstitution of L-Trp to L-4-Cl-Kyn. Genes encoding Tar13, 15, and 16 were individually cloned and expressed in *Escherichia coli* (Figure S12), while Tar14 was expressed in *S. coelicolor* CH999 (Figure S3).^[20] However, no yellow color associated with flavin binding was observed for Tar14, suggestive of either enzyme misfolding or a weak binding affinity.^[17,21] Upon incubation of Tar14 with flavin and a flavin reductase system (Figure 2B, Supplementary Information),^[22] we observed conversion of L-Trp to L-6-Cl-Trp as confirmed by high resolution mass spectrometry (HRMS) and NMR characterization of the purified product (Supplementary Information). Kinetic parameters of Tar14 with L-Trp were determined: $k_{cat}=0.4 \text{ min}^{-1}$, $K_M=12 \text{ }\mu\text{M}$, $k_{cat}/K_M=0.03 \text{ min}^{-1}\mu\text{M}^{-1}$, and are consistent with other characterized FDHs (Figures S6–S8, Table S6).^[23]

We next probed the substrate specificity of Tar14 towards different halide partners (Figure 2B, Table 1). Tar14 readily brominated L-Trp, however, it exhibited an erosion of regioselectivity, producing a 1:5 mixture of L-5-Br-Trp (**8**) and L-6-Br-Trp (**9**) as determined by HRMS and retention time comparison with commercial standards (Figure 2B, Figure S11). No iodinated tryptophan products were detected when incubated with iodide. To further investigate its biocatalytic halogenation potential, Tar14 was interrogated with a library of Trp derivatives (Table 1, Figures S16-S21, Table S7). Tar14 was capable of generating a wide variety of dihalogenated Trp species by accepting monohalogenated substrates. Previously, only the kutzneride FDH KtzR was shown to have L-7-Cl-Trp as its preferred substrate yielding L-6,7-diCl-Trp,^[24] while FDH KrmI from a sponge metagenome was able to chlorinate L-7-F-Trp,^[25] albeit at trace level.

We solved the X-ray crystal structure of Tar14 with bound flavin cofactor to a resolution of 1.74 Å (PDB: 6NSD) using the structure of C6 Trp halogenase Th-Hal (PDB: 5LV9, 73% identity)^[23] as a molecular replacement model (Supplementary Information, Table S5). Two protomers were observed in the asymmetric unit, consistent with the homodimeric form of Tar14 in solution (Figure S3). Each monomer adopts the classical FDH fold comprised of pyramid-like and box-shaped domains (Figure 3A).^[21] Catalytic lysine and glutamate residues identified for all characterized FDHs, remain conserved in Tar14. Bioinformatic analysis of Tar14 and other characterized Trp FDHs clearly shows existence of two subtypes of C6 halogenases: ThaI^[26] and BorH^[27] are closely related to C7 Trp halogenases, while Tar14, together with SttH,^[28] Th-Hal,^[23] and KtzR,^[24] forms a separate clade on the phylogenetic tree, and shows more sequence and structural similarity to C5 Trp halogenase PyrH^[29] (Figures S1, S2, S4, Table S4). Superimposition of Tar14 with related Th-Hal and SttH structures shows conservation of proposed active site residues (Figure 3B). However, structural superimposition with the phylogenetically distinct ThaI reveals that active site of these two enzymes are formed by different protein regions (Figure 3): residues of L-Trp interacting region β of ThaI do not have equivalents in Tar14, while Tar14 residues of regions γ and δ , positioned in the vicinity of the proposed active site, are missing in ThaI. In light of the observed substrate flexibility of Tar14, we looked for distinct structural and sequence features of Tar14 in comparison to SttH, Th-Hal, and KtzR. Sequence alignment superimposed onto the Tar14 structure showed that the putative substrate binding region remains conserved among these enzymes, and amino acid variations in Tar14 are distantly located from the putative active site (Figure S5).

We next examined the activity of TDO Tar13. Incubation of Tar13 with L-6-Cl-Trp (**7**) resulted in its complete conversion into a new early eluting compound (Figure 2C). HRMS and NMR data confirmed that the new peak corresponded to *N*-formyl-L-4-Cl-Kyn (**10**) (Supplementary Information). Kinetic parameters of Tar13 with L-6-Cl-Trp were determined: $k_{\text{cat}}=0.03 \text{ s}^{-1}$, $K_{\text{M}}=112.3 \text{ }\mu\text{M}$, $k_{\text{cat}}/K_{\text{M}}=0.27 \text{ min}^{-1}\text{mM}^{-1}$ (Figure S14). Upon mildly acidic purification conditions, **10** showed partial deformylation to L-4-Cl-Kyn (**1**). Therefore, to test the activity of KF Tar16, we performed a coupled Tar13/Tar16 assay in which the substrate for Tar16 was generated in situ (Supplementary Information). Addition of Tar16 to the reaction resulted in full conversion of **7** to **1**, thus confirming the role of Tar16 in the biosynthesis of **1**. We additionally explored the possibility of directly converting

L-Trp to L-4-Cl-Kyn in a one-pot reaction. The expected product was detected, however, the production of L-4-Cl-Kyn remained below 1% largely due to the incompatibility of optimal assay conditions for each individual enzyme in vitro (Figure 2C, Supplementary Information).

When we tested L-Trp as a substrate for Tar13, we only measured trace activity. This stark difference in the substrate preference of Tar13 was illuminated in a comparative in vitro substrate consumption assay of L-Trp versus L-6-Cl-Trp (Figure S15). Tar13's preference for the halogenated substrate was clearly evident by the slow rate of L-Trp consumption and failure to achieve its complete conversion. Bioinformatic analysis of the draft genome sequence of *S. sp.* CNQ-490 revealed a second pair of TDO/KF enzymes with less than 30% identity to Tar13/Tar16 and that are likely associated with L-Trp metabolism (Figures S32, S33). We hypothesize that Tar13 and Tar16 diverged from catabolic TDOs and KFs, respectively, and coevolved to serve a specialized role in L-4-Cl-Kyn biosynthesis after gene duplication. Collectively, our results indicate that Tar13 and Tar16 are the first representatives of their enzyme families to prefer chlorinated substrates.

We further probed Tar13 and Tar16 activity with a variety of substrate analogues (Table 1) and identified a preference of these enzymes towards C6 halogenated Trp derivatives (Figures S22-S25, Table S7). Phylogenetic analysis revealed that Tar13 and Tar16 are evolutionarily distinct from catabolic TDO and KFs, respectively (Figures S30, S31). Interestingly, they also branch out from other BGC-associated enzymes and form a separate clade with uncharacterized homologs. Inspection of gene neighborhoods of these homologs revealed nonribosomal peptide synthetase (NRPS) BGCs that also contain putative Trp FDH, KF, and adenylation (A) domain with predicted specificity towards Kyn (Table S9). This observation suggests halogenated kynurenine residues may be more widespread than previously thought in peptide natural products, and that Tar13/Tar16 sequences may be convenient "search hooks" for their discovery.

The in vitro substrate flexibilities of Tar13 and Tar16 encouraged us to probe whether analogous promiscuity is retained in vivo. The incorporation of Trp and Kyn derivatives additionally relies on the relaxed specificity of the corresponding NRPS A domains (A₁ and A₁₃). We fed a variety of Trp derivatives (Table 1) to *S. coelicolor* M1146-*tarM1 tar14*. Analysis of LC-HRMSⁿ data showed that all analogues, apart from **12**, were incorporated into residue-1 by A₁ (Table 1, Figures S26-S29, Table S8). However, we observed limited incorporation of non-native Kyn derivatives at residue-13 by A₁₃. This mirrors the in vitro activities of Tar13/Tar16, suggesting that the inability to generate corresponding Kyn derivatives in vivo likely precludes formation of disubstituted taromycins. Especially pleasing was the incorporation of fluorinated amino acids with yields close to taromycin production level (Figure 4, Table 1). Addition of fluorine is an important modification in medicinal chemistry that often results in improved selectivity, stability, and cell permeability of the therapeutically relevant compounds.^[30] We generated eight analogues of taromycin (four each of the **2** and **3** series) that contain either one or two fluorine substitutions and are presently exploring yield optimization and bioactivity testing.

In summary, we genetically and biochemically validated the three-step enzymatic route from L-Trp to L-4-Cl-Kyn. We anticipate that these enzymes will find utility as biocatalysts, especially when combined with enzyme engineering, and are a valuable addition to the toolkit for potential chemoenzymatic synthesis of halogenated aromatic molecules. Importantly, given the valuable therapeutic properties of L-4-Cl-Kyn and its ability to readily cross the blood-brain barrier, Tar13-16 enzymes represent an exciting opportunity for development as a microbiome-based therapy^[31] for the treatment of neurological disorders.^[32]

Supplementary Material

Refer to Web version on PubMed Central for supplementary material.

Acknowledgements

This work was supported by NIH grant R01-GM085770 to B.S.M., the Simons Foundation Fellowship of the Life Science Research Foundation to J.R.C., an NSERC postdoctoral fellowship to S.M.K.M., São Paulo Research Foundation FAPESP Proc. 2016/25735-1 to R.S. We thank Dr. P. Jensen and Dr. W. Fenical for *S. sp.* CNQ-490, Dr. M. Bibb for *S. coelicolor* M1146, Dr. S. Nair for PtdH and SsuE expression plasmids, Dr. P. Leadlay for pCJW93 and *S. coelicolor* CH999. We thank Dr. J. Noel and Dr. G. Louie for providing beamtime and assistance with beamline operation.

References

- [1]. Yaksh TL, Schwarcz R, Snodgrass HR, J. Pain 2017, 18, 1184–1196. [PubMed: 28428091]
- [2]. Vécsei L, Szalárdy L, Fülöp F, Toldi J, Nat. Rev. Drug Discov 2013, 12, 64–82. [PubMed: 23237916]
- [3]. Salituro FG, Tomlinson RC, Baron BM, Palfreyman MG, McDonald IA, Schmidt W, Wu HQ, Guidetti P, Schwarcz R, J. Med. Chem 1994, 37, 334–336. [PubMed: 8308859]
- [4]. Varasi M, Della Torre A, Heidempergher F, Pevarello P, Speciale C, Guidetti P, Wells D, Schwarcz R, Eur. J. Med. Chem 1996, 31, 11–21.
- [5]. Reynolds KA, Luhavaya H, Li J, Dahesh S, Nizet V, Yamanaka K, Moore BS, J. Antibiot 2018, 71, 333–338. [PubMed: 29184121]
- [6]. Yamanaka K, Reynolds KA, Kersten RD, Ryan KS, Gonzalez DJ, Nizet V, Dorrestein PC, Moore BS, Proc. Natl. Acad. Sci. U.S.A 2014, 111, 1957–1962. [PubMed: 24449899]
- [7]. Alferova VA, et al., Amino Acids 2018, 50, 1697–1705. [PubMed: 30178101]
- [8]. Schwarcz R, Curr. Opin. Pharmacol 2004, 4, 12–17. [PubMed: 15018833]
- [9]. Kurnasov O, Jablonski L, Polanuyer B, Dorrestein P, Begley T, Osterman A, FEMS Microbiol. Lett 2003, 227, 219–227. [PubMed: 14592712]
- [10]. Nozaki M, Ishimura Y, Biochem. J 1972, 128, 24P–25P.
- [11]. Sheoran A, King A, Velasco A, Pero JM, Garneau-Tsodikova S, Mol. BioSyst 2008, 4, 622–628. [PubMed: 18493661]
- [12]. Hitchcock MJM, Katz E, Arch. Biochem. Biophys 1988, 261, 148–160. [PubMed: 3341771]
- [13]. Keller U, Lang M, Crnovcic I, Pfennig F, Schauwecker F, J. Bacteriol 2010, 192, 2583–2595. [PubMed: 20304989]
- [14]. Zhang C, Kong L, Liu Q, Lei X, Zhu T, Yin J, Lin B, Deng Z, You D, PLoS One 2013, 8, e56772. [PubMed: 23437232]
- [15]. Brown D, Hitchcock MJ, Katz E, Can. J. Microbiol 1986, 32, 465–472. [PubMed: 2425918]
- [16]. Dorrestein PC, Yeh E, Garneau-Tsodikova S, Kelleher NL, Walsh CT, Proc. Natl. Acad. Sci. U.S.A 2005, 102, 13843–13848. [PubMed: 16162666]
- [17]. Ortega MA, et al., ACS Chem. Biol 2017, 12, 548–557. [PubMed: 28032983]

- [18]. Liu Y, Tao W, Wen S, Li Z, Yang A, Deng Z, Sun Y, *mBio* 2015, 6, e01714–e01715. [PubMed: 26556277]
- [19]. Gomez-Escribano JP, Bibb MJ, *Microb. Biotechnol* 2011, 4, 207–215. [PubMed: 21342466]
- [20]. Wilkinson CJ, Hughes-Thomas ZA, Rowe CJM, Böhm I, Deacon M, Wheatcroft M, Wirtz G, Staunton J, Leadlay P, *J. Mol. Microbiol. Biotechnol* 2002, 4, 417–426. [PubMed: 12125822]
- [21]. Dong C, Flecks S, Unversucht S, Haupt C, van Pée K-H, Naismith JH, *Science* 2005, 309, 2216–2219. [PubMed: 16195462]
- [22]. Gamal AE, et al., *Proc. Natl. Acad. Sci. U.S.A* 2016, 113, 3797–3802. [PubMed: 27001835]
- [23]. Menon BRK, Latham J, Dunstan MS, Brandenburger E, Klemstein U, Leys D, Karthikeyan C, Greaney MF, Shepherd SA, Micklefield J, *Org. Biomol. Chem* 2016, 14, 9354–9361. [PubMed: 27714222]
- [24]. Heemstra JR, Walsh CT, *J. Am. Chem. Soc* 2008, 130, 14024–14025. [PubMed: 18828589]
- [25]. Smith DRM, Uria AR, Helfrich EJN, Milbredt D, van Pée K-H, Piel J, Goss RJM, *ACS Chem. Biol* 2017, 12, 1281–1287. [PubMed: 28198609]
- [26]. Moritzer A-C, Minges H, Prior T, Frese M, Sewald N, Niemann HH, *J. Biol. Chem* 2018, jbc.RA118.005393.
- [27]. Chang F-Y, Brady SF, *Proc. Natl. Acad. Sci. U.S.A* 2013, 110, 2478–2483. [PubMed: 23302687]
- [28]. Shepherd SA, Menon BRK, Fisk H, Struck A-W, Levy C, Leys D, Micklefield J, *ChemBioChem* 2016, 17, 821–824. [PubMed: 26840773]
- [29]. Zhu X, De Laurentis W, Leang K, Herrmann J, Ihlefeld K, van Pée K-H, Naismith JH, *J. Mol. Biol* 2009, 391, 74–85. [PubMed: 19501593]
- [30]. Müller K, Faeh C, Diederich F, *Science* 2007, 317, 1881. [PubMed: 17901324]
- [31]. Isabella VM, et al., *Nature Biotechnol* 2018, 36, 857–864. [PubMed: 30102294]
- [32]. Kennedy PJ, Cryan JF, Dinan TG, Clarke G, *Neuropharmacology* 2017, 112, 399–412. [PubMed: 27392632]

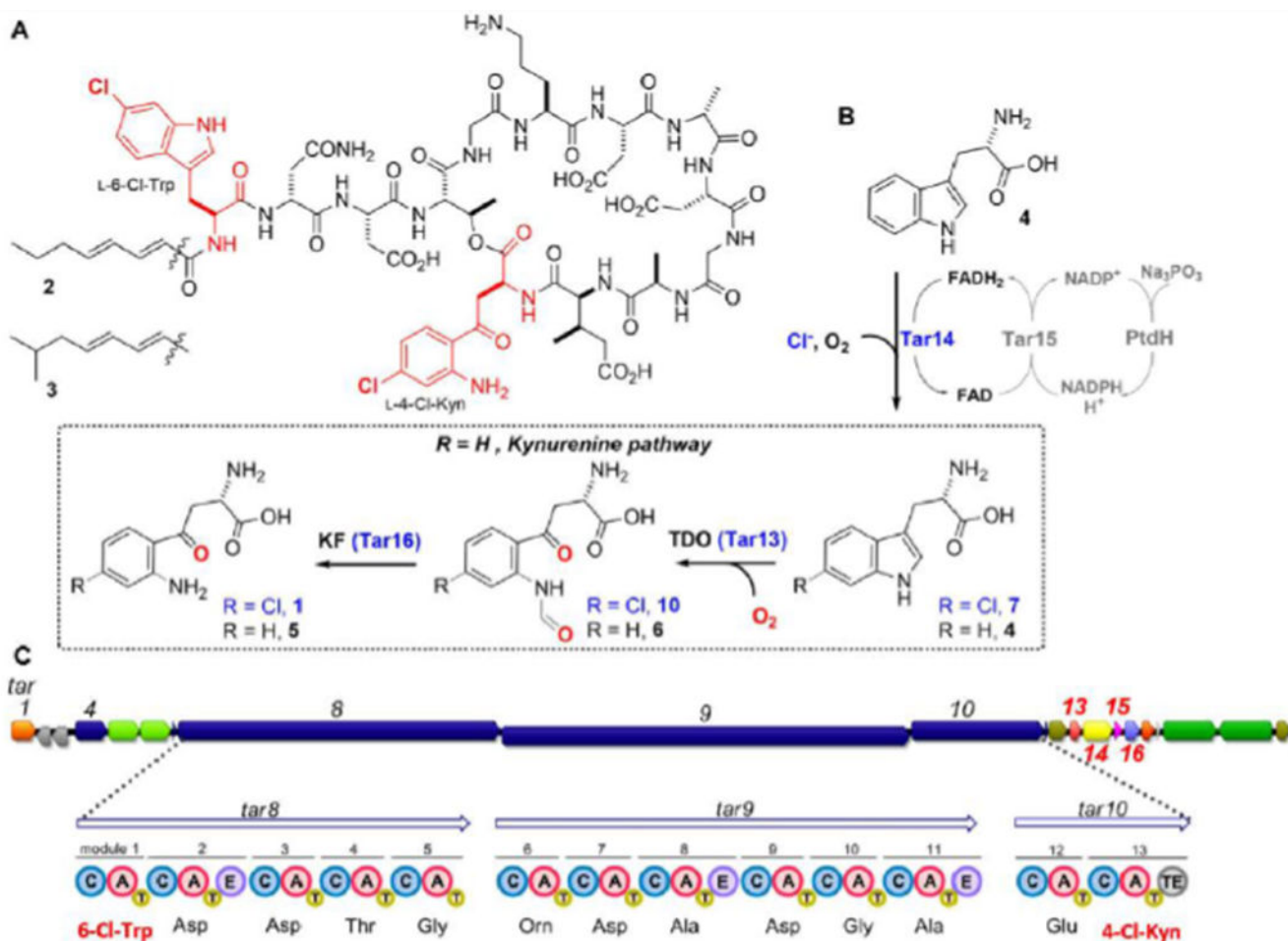


Figure 1.

A. Chemical structures of taromycins A (2) and B (3). **B.** Proposed enzymatic route from L-Trp (4) to L-4-Cl-Kyn (1). **C.** Gene organization of the taromycin BGC; *tar13,14,15,16* gene numbers are labeled red.

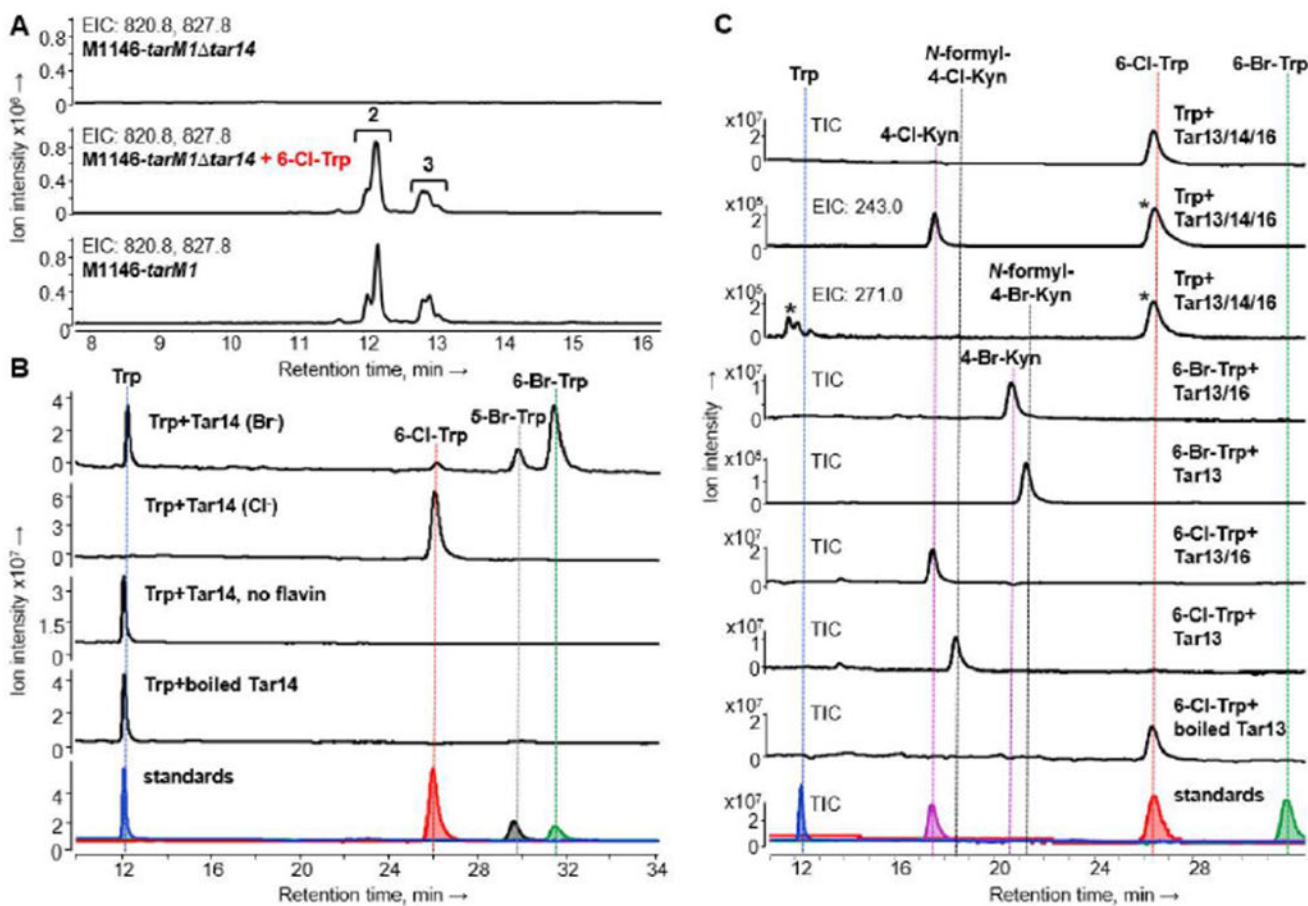


Figure 2.

A. LCMS extracted ion chromatograms (EIC) showing recovery of taromycin production by *S. coelicolor* M1146-*tarM1 tar14* mutant fed with 6-Cl-Trp; m/z $[M+2H]^{2+}$ 820.8 corresponds to taromycin A (**2**), m/z $[M+2H]^{2+}$ 827.8 – taromycin B (**3**). **B.** Total ion chromatograms (TIC) of Tar14-catalyzed halogenation of L-Trp. **C.** TIC and EIC confirming activity of Tar13 and Tar16, and one-pot conversion of L-Trp to L-4-Cl-Kyn. * not relevant to the reaction product; m/z $[M+H]^+$ 271.0 corresponds to N-formyl-L-4-Cl-Kyn, 243.0 – L-4-Cl-Kyn.

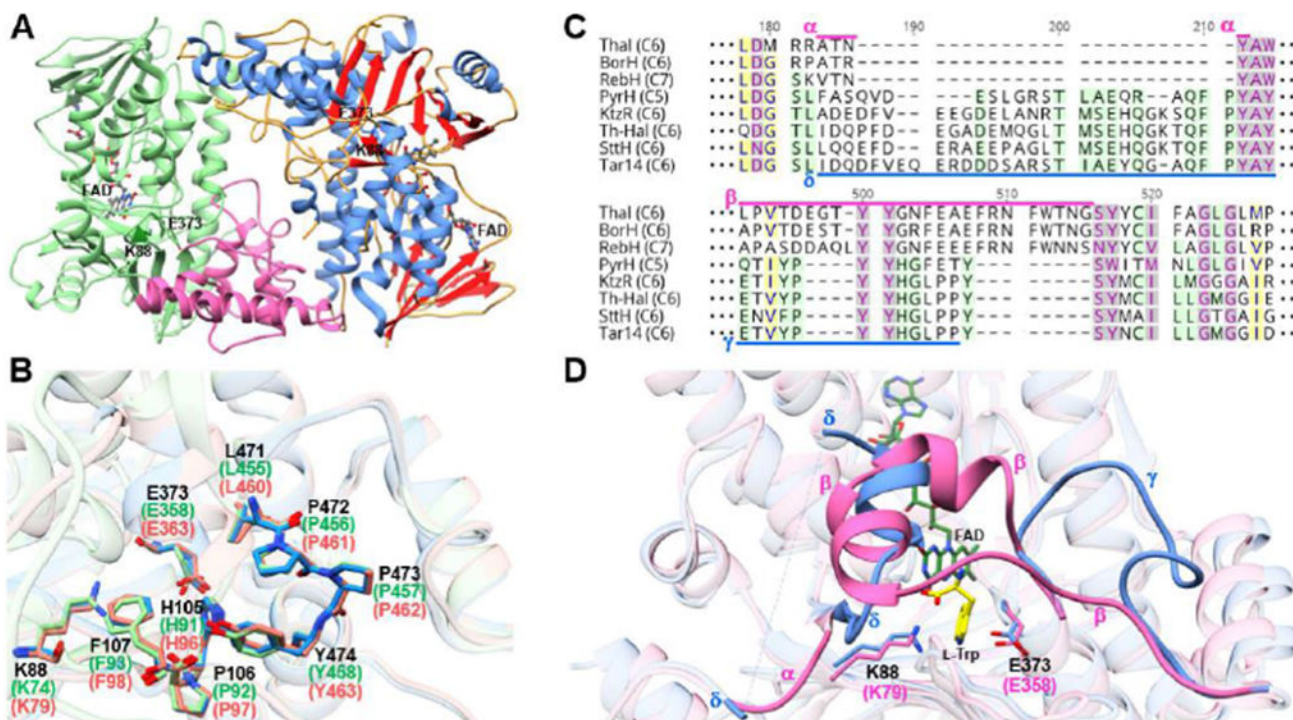


Figure 3.

A. Cartoon representation of the Tar14 structure. Monomer on the left is colored by domains: green – box-shaped domain, pink – pyramid domain; monomer on the right is colored by secondary structure: α -helices – blue, β -sheets – red, flexible loops – sand. Flavin molecules and catalytic K88 and E373 residues are labeled. **B.** Superimposition of putative active site residues of Tar14 (blue), Th-Hal (green), and SttH (salmon). **C.** Protein sequence alignment of Tar14 and selected Trp FDHs. Residues that form the active site in Thal are highlighted by pink lines, sequences surrounding the putative active site in Tar14 – blue lines. **D.** Superimposition of Tar14 (blue) and Thal (pink) structures illustrating difference in arrangement of the putative active site. Greek letters correspond to the respective sequence regions from the alignment above.

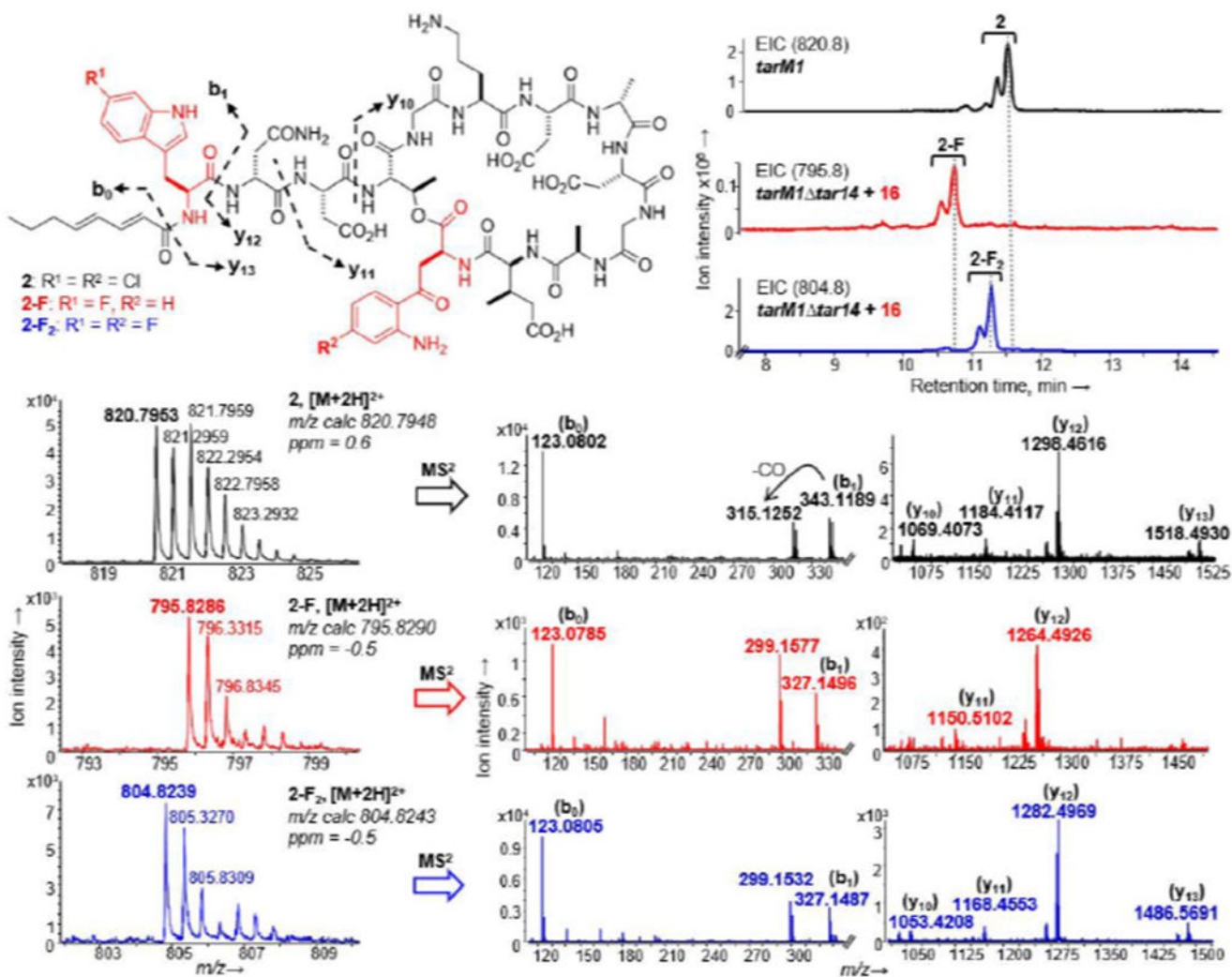
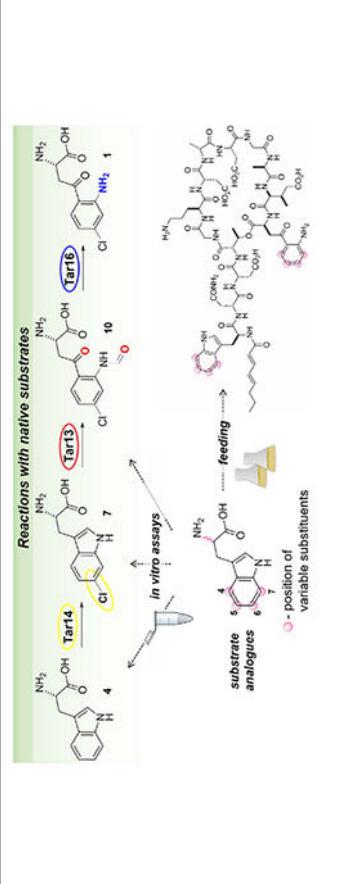


Figure 4. LC/ESI-Q-TOF MS² analysis of mono- (**2-F**, red) and di-fluorinated (**2-F₂**, blue) analogues of taromycin A (**2**) and their comparison to **2** (black).

Table 1.

Evaluation of L-4-Cl-Kyn biosynthesis enzymes against a panel of non-native substrate analogues.



| Substrate | Enzyme assays, % conversion | | | | Feeding, % incorporation* | |
|--------------------------------|-----------------------------|-----------|-------|--------|---------------------------|---|
| | Tar14, Cl | Tar14, Br | Tar13 | Tar16# | A ₁ domain | A ₁ +A ₁₃ domains |
| 1, L-4-Cl-Kyn | <1 | 5 | nt | nt | nt | nt |
| 4, L-Trp | 100 | 100 | 15 | 100 | - | <5 |
| 5, L-Kyn | 30 | 30 | nt | nt | nt | nt |
| 7, L-6-Cl-Trp | - | <5 | 100 | 100 | - | 100 |
| 8, L-5-Br-Trp | <1 | - | <1 | 100 | 50 | - |
| 9, L-6-Br-Trp | - | <1 | 100 | 100 | - | 20 |
| 11, D-Trp | 15 | 20 | <1 | 40 | - | - |
| 12, L-4-Br-Trp | <1 | <5 | - | nt | - | - |
| 13, L-7-Br-Trp | 100 | 100 | - | nt | <5 | - |
| 14, D/L-5-Cl-Trp | <1 | <1 | <1 | 100 | 30 | - |
| 15, D/L-4-F-Trp | 10 | 15 | - | nt | 15 | 15 |
| 16, D/L-6-F-Trp | 25 | 25 | 5 | 100 | <5 | 90 |
| 17, D/L-4-CH ₃ -Trp | 100 | 75 | - | nt | 40 | - |
| 18, D/L-5-CH ₃ -Trp | 50 | 25 | <1 | 70 | 35 | - |
| 19, L-5-CH ₃ O-Trp | <1 | <5 | <1 | 100 | 15 | - |
| 20, L-5-OH-Trp | 5 | <1 | - | nt | 10 | - |

| Substrate | Enzyme assays, % conversion | | | | Feeding, % incorporation* | |
|--|-----------------------------|------------------------|-------|--------------------|---------------------------|---|
| | Tar14, Cl ⁻ | Tar14, Br ⁻ | Tar13 | Tar16 [#] | A ₁ domain | A ₁ +A ₁₃ domains |
| 21 , D/L-5-NO ₂ -Trp | - | - | - | - | 60 | - |
| 22 , serotonin | - | - | - | - | nt | nt |
| 23 , L-tyrosine | - | - | nt | nt | nt | nt |
| 24 , L-phenylalanine | - | - | nt | nt | nt | nt |

nt – not tested; «-» – no activity;

[#] substrates generated in situ by Tar13;

* judged by comparison to tryptophan yields by *S. coelicolor*M1146-*tarM1*.